Struct Multidisc Optim 22, 167–176

Constrained adaptive topology optimization for vibrating shell structures

F. Belblidia and S. Bulman

Abstract This paper describes an algorithm for structural topology optimization entitled Constrained Adaptive Topology Optimization or CATO which is applied here to produce the optimum design of shell structures under free vibration conditions. The algorithm, based on an artificial material model and an updating scheme, combines ideas from the more mathematically rigorous homogenization (h) methods and the more intuitive evolutionary (e) methods. Thus, CATO can be seen as a hybrid h/e method. The optimization problem is defined as maximizing or minimizing a chosen frequency with a constraint on the structural volume/mass by redistributing the material through the structure. The efficiency of the proposed algorithm is illustrated through several numerical examples.

Key words free vibration, shells, topology optimization, artificial material

1 Introduction

In structural topology optimization three major techniques have emerged, they have some common aspects such as the material format, the iterative improvement scheme and the constraint satisfaction strategy. They can be classified as follows.

- Homogenization methods (h) use the optimality criteria algorithm based on Kuhn-Tucker conditions. The material is represented by a sponge-like material with infinitely many micro-scale cells with voids. Depending on the cell used to define the material model, we have rank-1 and rank-2 models, the square microcell with a rectangular void (Bendsøe and Kikuchi 1998) and finally the artificial material model or SIMP method (Zhou and Rozvany 1991; Rozvany *et al.* 1992). The optimization process is achieved by variation of the porosity of the sponge-like material throughout the structure.
- Evolutionary methods (e) are an intuitive engineering approach based on the fully stressed design techniques. In this case inefficient material is removed from the design domain to allow the emergence of a new topology. The removal process can be achieved by either the hard-kill/soft-kill methods (Hinton and Sienz 1995) or by the ESO technique (Xie and Steven 1997).
- Hybrid methods (h/e) which contain attributes of both (e) and (h) methods in differing degrees. The CATO algorithm belongs to this class of methods.

The structural response to dynamic loading depends, to a large extent, on the first few natural frequencies of the structure. It is often necessary to shift the fundamental or several lower frequencies of a structure away from the frequency range of a dynamic loading to avoid excessive vibrations of the structure. The natural frequencies of a structure represent, in fact, the dynamic characteristics of the structure and therefore play an important role in design optimization techniques because the dynamic response of the structure is controlled by its dynamic characteristics.

A great deal of research focused on structural optimization under dynamic loading conditions has been conducted during the past three decades. Most of the work is conducted on structural optimization with dynamic frequency constraints. Starting with the work of (Olhoff 1970, 1974) on optimal design of vibrating plates, a literature survey (Grandhi 1993) covers most of the work in this area. Recently the application of the homogenization method has been introduced with success in topology optimization of structural dynamic analy-

Received February 17, 2000

F. Belblidia and S. Bulman

Department of Civil Engineering, University of Wales, Swansea, UK
e-mail: F.Belblidia@Swansea.ac.uk
S.D.Bulman@Swansea.ac.uk

sis (Diáz and Kikuchi 1992; Ma *et al.* 1993; Tenek and Hagiwara 1993). Finally the evolutionary structural optimization method (Xie and Steven 1996, 1997) is used to solve natural frequency optimization for vibrating structures.

In the present paper, the CATO algorithm, which has been applied to the topology optimization of structures under static conditions (Bulman and Hinton 1999; Belblidia *et al.* 2000) is extended to structures under free vibration conditions.

The main purpose of the CATO algorithm is to find an optimal structural topology by using the structural material more efficiently and satisfying some basic requirements for a structural design. More specifically, the main purpose of the natural frequency structural optimization is to find an optimum structural topology, which corresponds to the minimum or maximum of a particular natural frequency of the structure and satisfies a structural volume/mass constraint. This is achieved by redistributing material within the structure creating zones of void (no material) and solid (material). This results in an optimum stiffening structural topology which is presented as a variable density plot. We ensure that the targeted structural volume is maintained during the complete iterative process, so that at each iteration step we have a valid solution.

The paper first introduces the optimization problem and the frequency sensitivity criterion. A detailed description of the CATO algorithm is then introduced where the single layered artificial material model is described, followed by a detailed explanation of the iterative material updating scheme process used within CATO. Finally, several examples are provided to demonstrate the use of the CATO algorithm in topology optimization of shell structures under free vibration conditions.

2
Frequency sensitivity criterion

To find the best location for the material at each iteration, a factor for each element in the structure is evaluated. This sensitivity factor, which indicates the influence the material has on the natural frequency of the structure, can be defined as follows.

The eigenvalue problem which define the dynamic behaviour of the structure is stated as

$$(\mathbf{K} - \omega_n^2 \mathbf{M})\ \mathbf{u}_n = 0\,, \tag{1}$$

where $\mathbf{K}$ and $\mathbf{M}$ are the global stiffness and mass matrices respectively, ω_n is the nth natural frequency and $\mathbf{u}_n$ is the corresponding eigenvector. The natural frequency ω_n and the corresponding eigenvalue $\mathbf{u}_n$ are related to each other by the Rayleigh quotient

$$\omega_n^2 = \frac{k_n}{m_n}\,, \tag{2}$$

in which the modal stiffness k_n and the modal mass m_n are defined as

$$k_n = \mathbf{u}_n^T \mathbf{K} \mathbf{u}_n\,, \quad \text{and} \quad m_n = \mathbf{u}_n^T \mathbf{M} \mathbf{u}_n\,. \tag{3}$$

The change in the frequency by the redistribution of material in the structure can be obtained by the sensitivity calculation of the frequency as

$$\Delta(\omega_n^2) = \frac{m_n \Delta k_n - k_n \Delta m_n}{m_n^2} = \frac{1}{m_n}(\Delta k_n - \omega_n^2 \Delta m_n)\,. \tag{4}$$

If an element e has be removed from the structure during the material redistribution scheme by creating an elemental void in the structure, the frequency sensitivity can be evaluated approximately by assuming that the eigenvector $\mathbf{u}_n$ has not been affected by this removal of that element (Grandhi 1993; Xie and Steven 1997), therefore

$$\Delta k_n = \mathbf{u}_n^{(e)^T} \Delta \mathbf{K}\ \mathbf{u}_n^{(e)} = -\mathbf{u}_n^{(e)^T} \mathbf{K}^{(e)}\ \mathbf{u}_n^{(e)}\,,$$

$$\Delta m_n = \mathbf{u}_n^{(e)^T} \Delta \mathbf{M}\ \mathbf{u}_n^{(e)} = -\mathbf{u}_n^{(e)^T} \mathbf{M}^{(e)}\ \mathbf{u}_n^{(e)}\,, \tag{5}$$

in which $\mathbf{K}^{(e)}$ and $\mathbf{M}^{(e)}$ are the stiffness and mass matrices of the removed element e, and $\mathbf{u}^{(e)}$ is the eigenvector of that element. The sensitivity of the frequency due to the removal of the eth element is obtain by substituting (5) into (4), so that

$$\Delta(\omega_n^2) = f^e = \frac{1}{m_n}\ \mathbf{u}_n^{(e)^T} \left(\omega_n^2 \mathbf{M}^{(e)} - \mathbf{K}^{(e)}\right)\ \mathbf{u}_n^{(e)}\,. \tag{6}$$

The sensitivity factor f^e is an indicator of the change in the natural frequency as a result of the change of the material amount in the element e. This factor is used as a criterion in the updating scheme used in CATO.

Note that the expression (6) of this factor can be simplified by omitting the modal mass m_n from (6) as m_n is the same for every element in the structure. Note also that the eigenvector $\mathbf{u}_n$ can be normalized by the mass matrix $\mathbf{M}$, in this case the modal mass becomes equal to unity. Note also that the summation of the sensitivity factor over all the elements is equal to zero which is useful for checking the correctness of the code.

3
Constrained topology optimization method

Let us describe the main features of the CATO method. Firstly the single layered artificial material model is introduced, followed by a detailed explanation of the iterative material updating scheme process. Finally, several ex-

amples are presented to show the performance of the proposed algorithm for shell structures under free vibration conditions.

3.1 Artificial material model

By considering structural topology optimization as a material distribution problem, the structure can be described by a discrete function χ, defined at each point $\mathbf{x}$ as

$$\chi(\mathbf{x}) = \begin{cases} 1 & \text{if } \mathbf{x} \in \Omega_s \quad \text{material} \\ 0 & \text{if } \mathbf{x} \in \Omega \backslash \Omega_s \quad \text{no material} \end{cases}, \tag{7}$$

where Ω is the design domain, Ω_s is the solid part of it and $\mathbf{x} \in \Omega$ is the vector of design variables.

If isotropic behaviour is assumed for the solid part of the structure, we can write

$$\rho(\mathbf{x}) = \chi(\mathbf{x})\rho^0\,, \quad \text{and} \quad \mathbf{D}(\mathbf{x}) = \chi(\mathbf{x})\mathbf{D}^0\,, \tag{8}$$

where ρ^0 and $\mathbf{D}^0$ are the density and elastic constitutive matrix, respectively, of the homogeneous solid.

For the numerical solution of the optimization problem, the discrete function χ causes solution difficulties (Bendsøe and Kikuchi 1998). One easy way to overcome these difficulties is to replace the discrete function χ by a continuous one ξ, where $0 \le \xi(x) \le 1$. For convenience we will assume that the material has a micro-cellular structure and each cell is a square with a square hole of side length a where $0 \le a \le 1$. Thus, in the present model

$$\xi(x) = 1 - a^2(x)\,. \tag{9}$$

Note that by changing the size of the square hole, which is used as a design variable, we are able to create a micro-cellular void ($a = 1$) or solid ($a = 0$). CATO uses this concept to redistribute material iteratively in the structure.

It is desirable to obtain a solution which only consists of solid and void regions. This allows a better approximation to condition (7). Hence a parameter μ can be included to penalize the intermediate values of $\xi(\mathbf{x})$ (Rozvany *et al.* 1992). Hence,

$$\rho(\mathbf{x}) = \xi(\mathbf{x})^\mu\rho^0\,, \quad \text{and} \quad \mathbf{D}(\mathbf{x}) = \xi(\mathbf{x})^\mu\mathbf{D}^0\,, \tag{10}$$

where the exponent $\mu > 1$ and is usually between 3 and 9.

Note that although we have assumed a micro-cellular material with square hole size a, we have approximated the resulting material behaviour as though it were isotropic (with a scaling factor) rather than truly orthotropic. There is, therefore, no dependency on the orientation of the square hole in the artificial material model unlike the case for the more conventional micro-cell model.

3.2 The CATO algorithm

For a chosen frequency ω_{par}, the result of the sensitivity factor values f^e for each element are obtained from a free vibration analysis at each iteration, CATO order these values according to the type of frequency optimization required

- in an ascending order of f^e for a frequency minimization problem, or
- in an ascending order of $-f^e$ for a frequency maximization problem. This allows the use of the same algorithm for both frequency minimization or maximization problem.

The CATO algorithm is now summarized in the following steps. Note that we have used the standard term "design" and "nondesign" domain to refer to zones in which the density parameters are allowed to change and zones where they are not.

1. Set up the design domain data, optimization data and FE model data including information defining the mesh, material properties, boundary conditions. Set iteration counter $i = 1$.
2. For the desired volume fraction, V_{fac}, initialize the material density parameters a_i^e for each element according to the expressions

$$a_i^e = \begin{cases} 0 & \text{if nondesign domain} \\ (1 - V_{fac})^{1/2} & \text{if design} \\ a_{pr} & \text{if prescribed.} \end{cases}$$

   Calculate the desired volume of the system V_{des} using

$$V_{des} = V_{fac} * \sum_{e=1}^{n} v^e$$

   where n is the number of elements present in the model and v^e is the volume of element e.
3. For the current a_i^e values evaluate the appropriate constitutive properties using an artificial material model, see Sect. 3.1.
4. Perform a free vibration analysis.
5. Order the elements according to their sensitivity factor values f^e.
6. From a specified volume preserving relationship $\Delta a_i^e(f^e)$ evaluate the change of the density parameters Δa_i^e for each element and update the density parameter so that $a_{i+1}^e = a_i^e + \Delta a_i^e$, see Sect. 3.3.
7. Given the new density parameters a_{i+1}^e, evaluate the overall structural volume of the system V_{sys}.
8. Check the requirement that $V_{sys}/V_{des} < V_{tol}$. If this condition is not satisfied, adjust a_{i+1}^e proportionately to obtain $V_{sys} = V_{des}$ and go to step 7.

9. If some convergence criterion is met continue to step 10, otherwise set $i = i + 1$ and return to step 3.
10. Post-process the results prior to visualization and then terminate the solution.

3.3 Material updating scheme for frequency optimization

The CATO algorithm uses an incremental relationship $\Delta a^e(f^e)$ to adjust the elemental material parameter a^e according to the element sensitivity factor value f^e related to the chosen frequency ω_{par}. A special feature of this relationship is that it is chosen so as to preserve the total volume of the structure during the optimization iterative process. Figure 1 shows an example of this relationship at two stages of the scheme. The function is composed a curve of the form $y = n^{p_{cur}}$ (n and p_{cur} are described later).

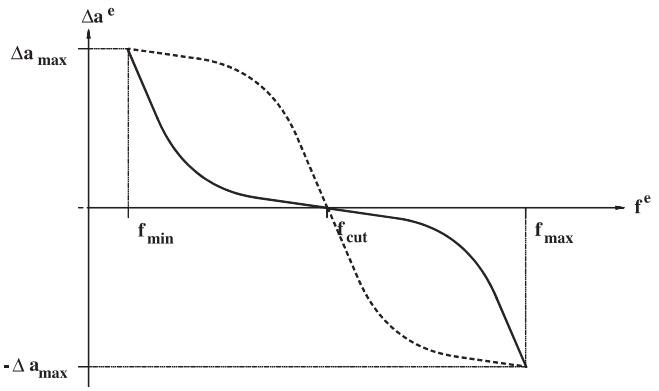

Fig. 1 Example of the relationship $\Delta a^e(f^e)$ at an early stage of the iterative scheme (solid line), and at an intermediate stage (dash line)

To define the curve some parameters are needed. If $\ell = [\ell^1, \ell^2, \ldots, \ell^n]^T$ is the list of n element numbers ordered as increasing f^e values for a frequency minimization problem or $-f^e$ for a maximization one, then three parameter values $f_{\min}$, $f_{\max}$ and f_{cut} are calculated as

$$f_{\min} = f^{(\ell^1)}\,, \quad f_{\max} = f^{(\ell^n)}\,, \quad f_{\text{cut}} = f^{(\ell^k)}\,, \tag{11}$$

where k satisfies the equation

$$\sum_{i=k}^{n} v^{\ell^i} = V_{des}\,, \tag{12}$$

and v^{ℓ^i} is the volume of element ℓ^i.

The change in the density parameter Δa_i^e for element e at iteration i is illustrated in Fig. 1 and is given by

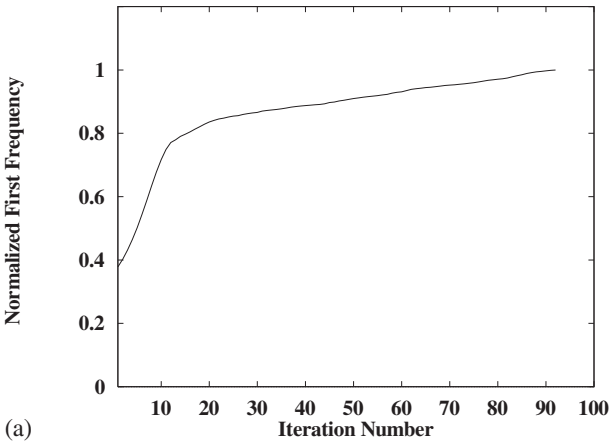

(a)

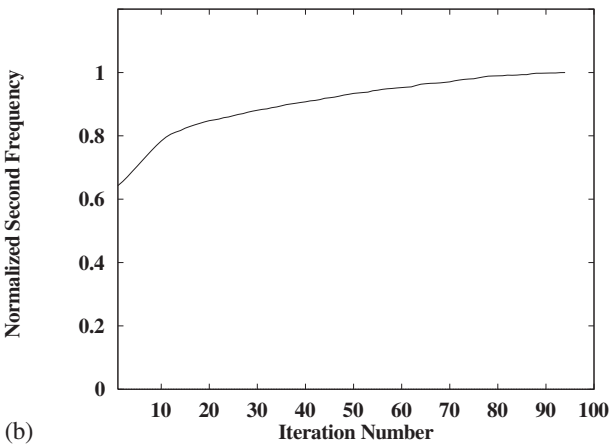

(b)

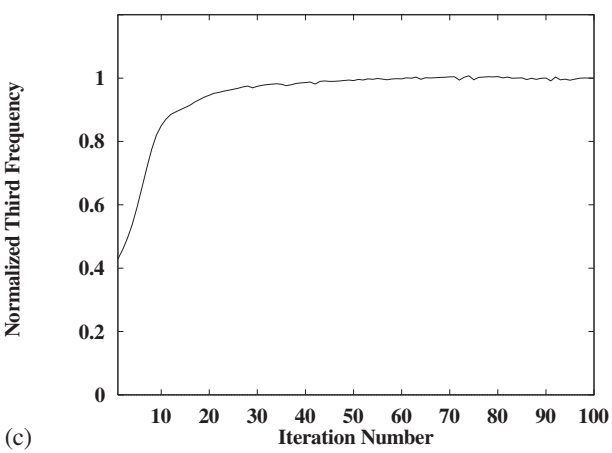

(c)

Fig. 2 Convergence of normalized frequency of a short beam example: (a) maximize the first frequency, (b) maximize the second frequency, (c) maximize the third frequency

$$\Delta a_i^e = f n^{p_{cur}}\,, \tag{13}$$

where

$$f = -\frac{f^e - f_{cut}}{|\, f^e - f_{cut}\,|}\,, \quad n = \frac{f^e - f_{cut}}{r}\,,$$

$$p_{cur} = p_{init} - ((i - 1.0) * iter)\,, \tag{14}$$

(a) (b) (c)

Fig. 3 Topology optimization results of a short beam example: (a) maximize the first frequency, (b) maximize the second frequency, (c) maximize the third frequency

and r is defined as

$$r = \begin{cases} f_{\max} - f_{cut} & \text{if } f^e > f_{cut} \\ f_{\min} - f_{cut} & \text{if } f^e \leq f_{cut}. \end{cases} \tag{15}$$

Three further parameters are specified by the user, they are:

(a) The maximum incremental density parameter $\Delta a_{\max}$ which governs the maximum allowable change in Δa^e at any one iteration cycle.
(b) The initial curve exponent parameter p_{init} determines the initial configuration of the curve.
(c) Finally, the iterative advancing parameter *iter* controls how the curve adapts through the iterative scheme.

Once the density parameters a_i^e for all elements in the design domain have been updated the volume of the new system is evaluated to check that the volume fraction constraint is not violated using the expression

$$V_{sys}/V_{des} < V_{tol}\,, \tag{16}$$

where V_{sys} is the current system volume, V_{des} is the desired system volume and V_{tol} is some allowable tolerance on the volume constraint.

If (16) is satisfied, then the algorithm can proceed to the next iteration. However, if (16) is not satisfied then the volume error for each element is calculated as

$$V_{err} = \frac{V_{sys} - V_{des}}{n}\,, \tag{17}$$

where n is the number of elements in the design domain. The new density parameter a_{i+1}^e for each element is then simply taken as

$$a_{i+1}^e = a_i^e + V_{err}\,. \tag{18}$$

3.4 Convergence

Two termination criteria are used in CATO process, if one of them is satisfied, the topology optimization is terminated. These criteria are:

1. A maximum number of iterations, k_{max}, can be provided by the user.

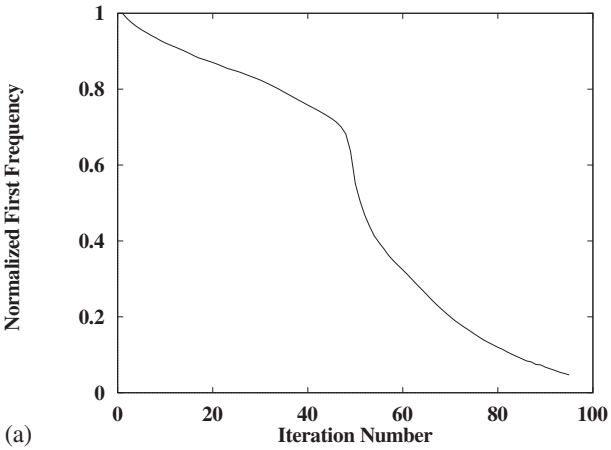

(a)

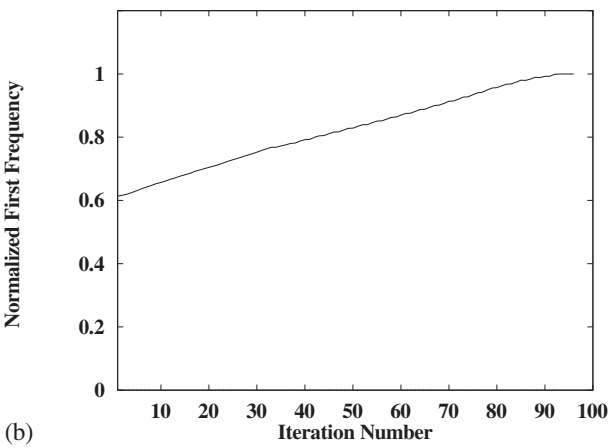

(b)

Fig. 4 Convergence of normalized frequency of a square 2D plate example: (a) minimize the first frequency, (b) maximize the first frequency

2. The frequency norm ($\mid {\omega_n}^k - {\omega_n}^{k-1} \mid / {\omega_n}^{k-1}$) between two subsequent topology optimization iterations $k-1$ and k may be examined and if it is smaller than a given value, then the program is terminated.

After convergence some post-processing of the results is conducted which included a thresholding technique in order to get a black and white topology image.

4 Examples

CATO has already been tested with success on topology optimization of shell structures under static conditions (Belblidia *et al.* 2000). Now CATO is illustrated for free

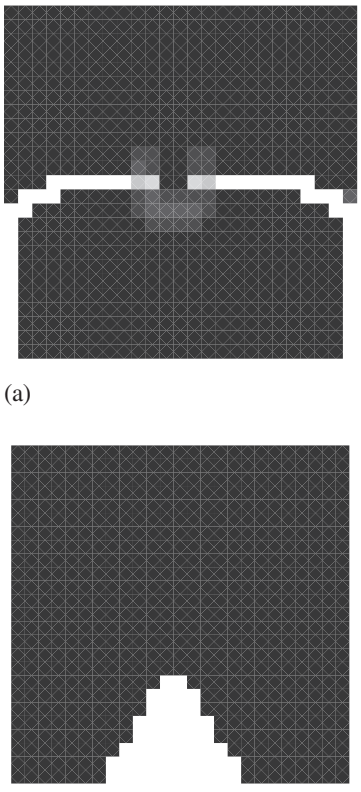

(a)

(b)

Fig. 5 Topology optimization results of a square 2D plate example: (a) minimize the first frequency, (b) maximize the first frequency

vibration conditions of shell structures under membrane behaviour in Sect. 4.1, bending behaviour in Sect. 4.2 and finally, Sect. 4.3 illustrates examples for general shell structures.

A single layered artificial material is considered and the common parameters used for the CATO algorithm in all examples are: maximum incremental density parameter $\Delta a_{\max} = 0.05$, the initial curve exponent parameter $p_{init} = 5.0$, and the iterative advancing parameter *iter* is 0.05. A maximum of 100 iterations is assumed with a convergence tolerance in the change of the frequency norm of 1%. For each example, the convergence history of the normalized chosen frequency is given with the optimum topology design. All units are assumed to be consistent. We should note that because we are using artificial material model, the frequency values obtained during the iterative process are normalized by their maximum value.

4.1 Plates under membrane behaviour

We now consider two plate examples under membrane behaviour. The first example is a short beam plate and the second is a square plate.

4.1.1 Short beam example

A short beam plate of dimensions 10×1 is clamped at its two opposite short sides. The example is taken from Xie and Steven (1997). The symmetric half of the plate is analysed using a structured FE mesh consisting of 50×10 quadrilateral nine noded elements. The problem data is: elastic modulus $E = 2.0 \times 10^5$, Poisson's ratio $\nu = 0.3$, mass density $\rho = 7000$, and the plate thickness $h = 0.1$. Three topology optimization problems are investigated, dealing with (a) the maximization of the first, (b) the second and finally (c) the third frequency using a volume fraction of $V_f = 90\%$ and a penalty exponent for the artificial material of $\mu = 3$.

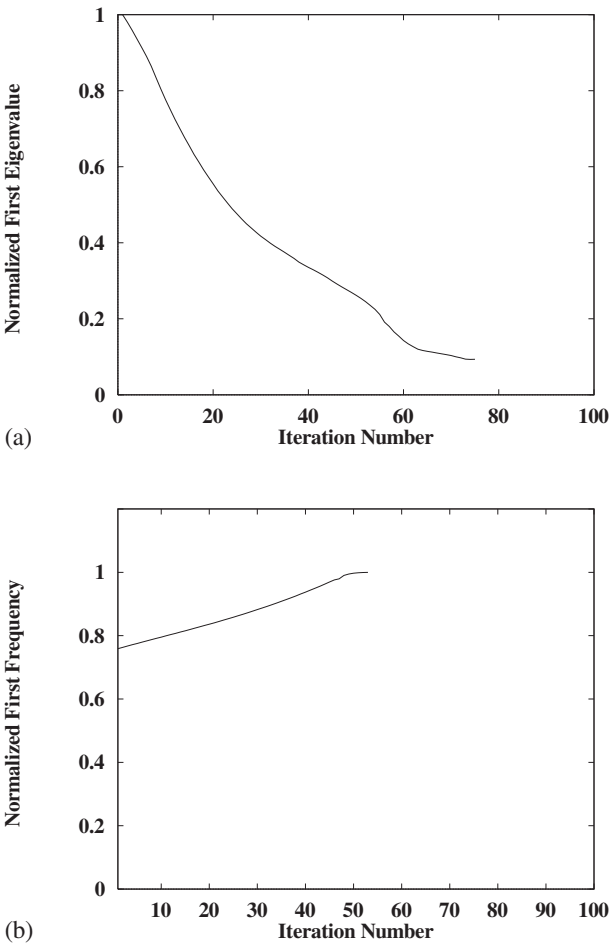

(a)

(b)

Fig. 6 Convergence of normalized frequency of a clamped square plate example: (a) minimize the first frequency, (b) maximize the first frequency

Figure 2 illustrates the variation of the normalized (a) first, (b) second and (c) third frequency with increasing number of iterations while Fig. 3 shows their respective optimal stiffening topologies for the whole plate. The first and second topology results are in good agreement with Xie and Steven (1997).

4.1.2
Square plate example

A square plate of dimension 10×10 is clamped at three sides as in Xie and Steven (1997). The whole plate is meshed with 25×25 nine noded elements. The problem data is: elastic modulus $E = 70\,000.0$, Poisson's ratio $\nu = 0.3$, mass density $\rho = 2700$, and the plate thickness $h = 0.01$. Two topology optimization problems are investigated dealing with (a) the minimization and (b) the maximization of the first frequency using a volume fraction of $V_f = 92\%$ and a penalty exponent for the artificial material of $\mu = 3$.

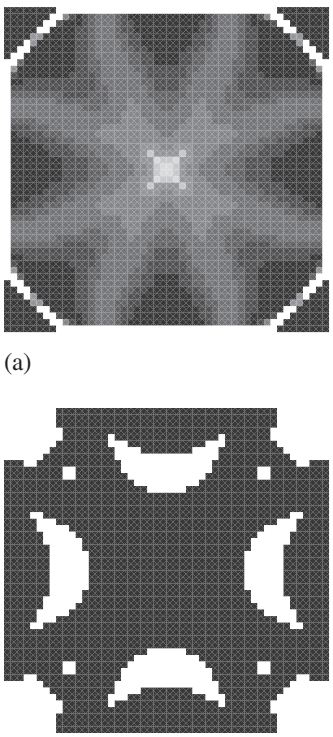

(a)

(b)

Fig. 7 Topology optimization results of a clamped square plate example: (a) minimize the first frequency, (b) maximize the first frequency

Figure 4 illustrates the variation of the normalized first frequency for case (a) and (b) respectively while Fig. 5 shows the respective optimal stiffening topologies. The topology results are in good agreement with Xie and Steven (1997). Note that when dealing with a frequency minimization, it can happen that the structure connectivity collapses leading to a nondefined structure. The user can stop the iterative process or a structural connectivity criterion can be introduced (Zhao and Steven 1996). In CATO when dealing with a minimization problem, no thresholding is used and therefore the final topology result is a grey scaled image.

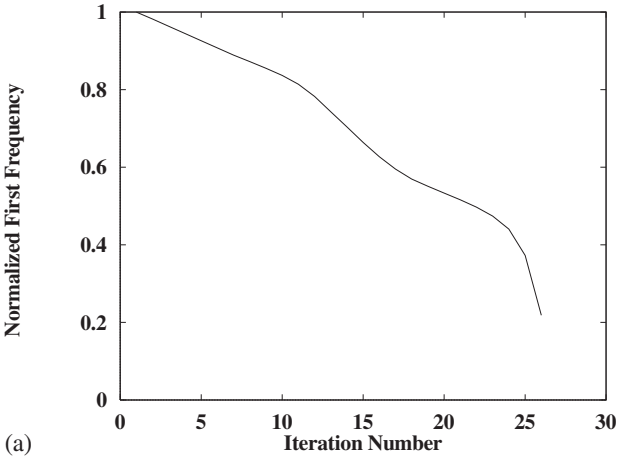

(a)

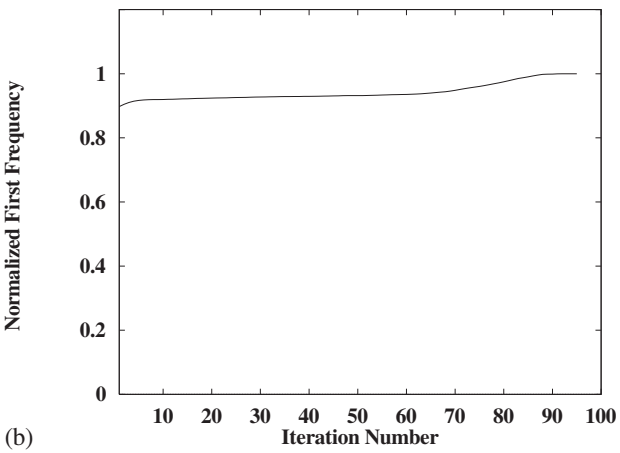

(b)

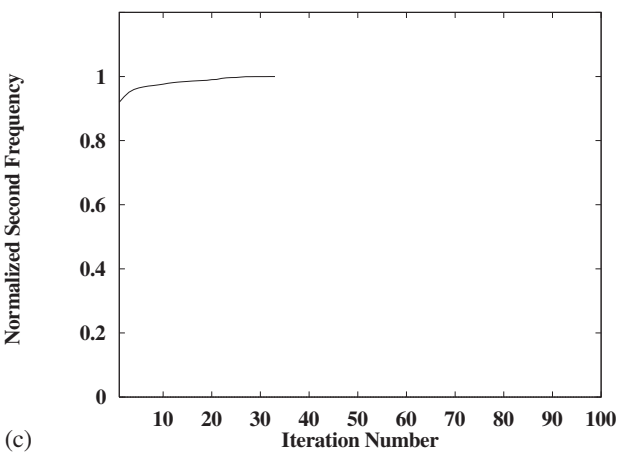

(c)

Fig. 8 Convergence of normalized frequency of a conoid shell example: (a) minimize the first frequency, (b) maximize the first frequency, (c) maximize the second frequency

4.2
Clamped square plate under bending behaviour

The free vibration topology optimization for a clamped supported on all four edges of a square plate under bending behaviour is now investigated.

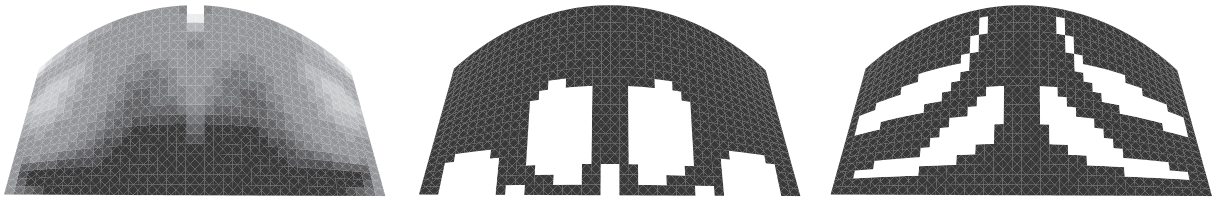

(a) (b) (c)

Fig. 9 Topology optimization results of a conoid shell example: (a) minimize the first frequency, (b) maximize the first frequency, (c) maximize the second frequency

A structured FE mesh consisting of 625 (25×25) quadrilateral nine noded shell elements is used to idealize the plate quadrant, and the plate side length $a = 10$. The problem data is: elastic modulus $E = 70\,000.0$, Poisson's ratio $\nu = 0.3$, mass density $\rho = 2700$, and the plate thickness $h = 0.01$.

The optimization problems are defined as (a) minimizing the first frequency or (b) maximizing it using a volume fraction of 75% and a penalty exponent of $\mu = 5$.

Figure 6 illustrates the variation of the normalized first frequency for case (a) and (b) respectively while Fig. 7 shows the respective optimal stiffening topologies for the whole plate. Note that if a thresholding is applied in case (a) the topology image becomes separated at the corners of the plate. Note also that that topology image for case (a) is the 'negative' image of case (b).

4.3 Shell structures

In the following two examples the optimization problems are defined as (a) minimizing the first frequency, (b) maximizing the first frequency and finally (c) maximizing the second frequency using a volume fraction of 75% and a penalty exponent of $\mu = 5$.

In the first example, only the symmetric quadrant of the shell is analysed, while for the second example a symmetric half is considered, however, in both examples the topology image shows the result for the whole shell structure.

For all examples a structured FE mesh consisting of 400 (20×20) quadrilateral nine noded shell elements is used to idealize the symmetric part of the shell considered.

In these examples the problem data is: elastic modulus $E = 70\,000.0$, Poisson's ratio $\nu = 0.3$, mass density $\rho = 2700$, and the plate thickness $h = 0.01$.

4.3.1 Conoid shell

In this example, the shell has three straight edges and a curved edge defined by the conoid parabolic surface

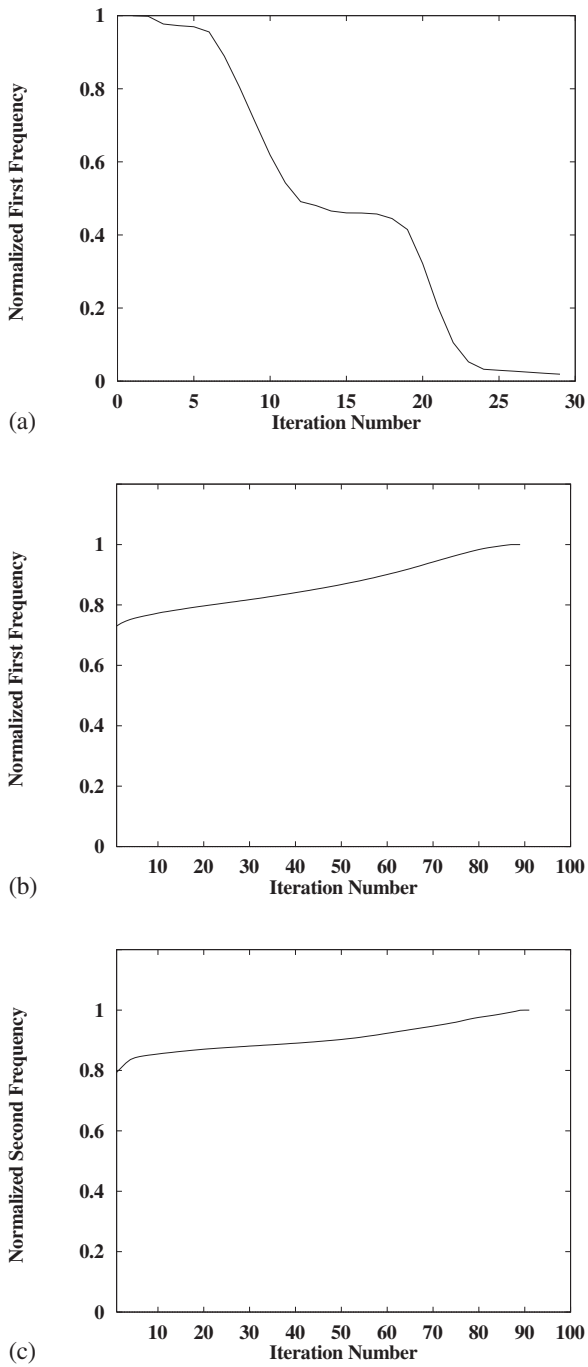

Fig. 10 Convergence of normalized frequency of a clamped EP shell example: (a) minimize the first frequency, (b) maximize the first frequency, (c) maximize the second frequency

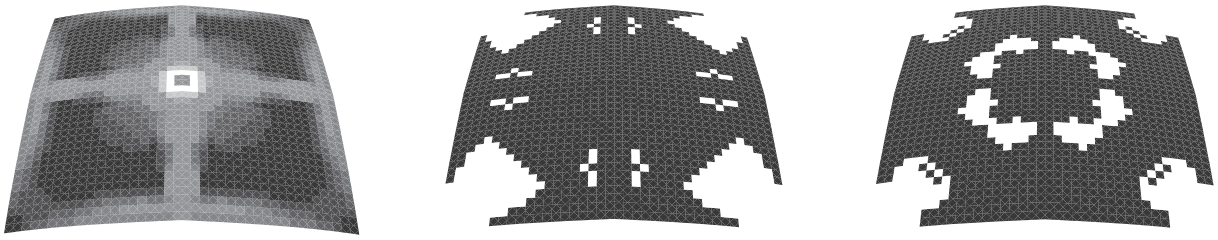

(a) (b) (c)

Fig. 11 Topology optimization results of a clamped EP shell example: (a) minimize the first frequency, (b) maximize the first frequency, (c) maximize the second frequency

$$z(x,y) = \frac{ky}{a} \times \left(1 - \frac{y^2}{a^2}\right) ,$$

where the curvature factor k is taken equal to 50.0 and the projection of the shell on the xy plane is a square of side length $a = 100$. The curved edge is aligned with the x-axis and the shell geometry is interpolated linearly along the y-axis. Both ends of the curved edge are supported by a hinge and the straight edge opposite to the curved edge is clamped. The other edges are free.

Figure 8 illustrates the variation of the normalized frequency for (a) minimized the first frequency, (b) maximized the first frequency and (c) maximized the second frequency respectively while Fig. 9 shows the respective optimal stiffening topologies for the whole shell.

4.3.2
Elliptic paraboloid (EP) shell with parabolic edges

The EP shell surface is obtained by translating a hogging parabola over another hogging parabola fixed in a vertical plane, while keeping the plane of the moving parabola vertical and at right angles to the plane of the fixed parabola. The surface equation can be expressed by

$$z(x,y) = \frac{k}{a^2}(x^2 + y^2) ,$$

where k is equal to 0.13 and the projection of the shell on the xy plane is a square of side length $a = 1$. The shell has a centrally applied point load and its four edges are clamped.

Figure 10 illustrates the variation of the normalized frequency for (a) minimized the first frequency, (b) maximized the first frequency and (c) maximized the second frequency respectively while Fig. 11 shows the respective optimal stiffening topologies for the whole shell.

5
Concluding remarks

This paper has illustrated the use of the CATO algorithm for topology optimization of shell structures under free vibration conditions. The algorithm combines ideas from both conventional H- and E-methods. Several examples are introduced and can be compared with previously known work with favourable results. No thresholding has been used with a frequency minimization problem to avoid the collapse of structural connectivities. We have noticed that for a minimization of a particular frequency, the topology image is the "negative" of the image of the maximization of that particular frequency.

Acknowledgements This paper is presented as a tribute to Prof. E. Hinton. The authors gratefully acknowledge the sponsorship provided by the EPSRC for the FIDO project.

References

Belblidia, F.; Bulman, S.; Hinton, E. 2001: Constrained adaptive topology optimization for shell structures. (under review)

Bendsøe, M.P.; Kikuchi, N. 1998: Generating optimal topologies in structural design using homogenization method. *Comp. Meth. Appl. Mech. Engng.* **71**, 197–224

Bulman, S.; Hinton, E. 1999: Constrained adaptive topology optimization of engineering structures. *Des. Opt.* **1**, 419–439

Diáz, A.R.; Kikuchi, N. 1992: Solution to shape and topology eigenvalue optimization problems using a homogenization method. *Int. J. Num. Meth. Engng.* **35**, 1487–1502

Grandhi, R.V. 1993: Structural optimization with frequency constraints – a review. *AIAA J.* **31**, 2296–2303

Hinton, E.; Sienz, J. 1995: Fully stressed topological design of structures using an evolutionary procedure. *Engineering Computational* **12**, 229–244

Ma, Z.D.; Kikuchi, N.; Cheng, H.C.; Hagiwara, I. 1993: Topology and shape optimization methods for structural dynamic problems. In: Pedersen, P. (ed.) *Optimal design with advanced materials*, pp. 247–261. Oxford: Elsevier

Olhoff, N. 1970: Optimal design of vibrating circular plates. *Int. J. Solids Struct.* **6**, 139–156

Olhoff, N. 1974: Optimal design of vibrating rectangular plates. *Int. J. Solids Struct.* **10**, 93–109

Rozvany, G.I.N.; Zhou, M.; Birker, T. 1992: Generalized shape optimization without homogenization. *Struct. Optim.* **4**, 250–252

Tenek, L.H.; Hagiwara, I. 1993: Static and vibrational shape and topology optimization using homogenization and mathematical programming. *Comput. Meth. Appl. Mech. Engng.* **109**, 143–154

Xie, Y.M.; Steven, G.P. 1996: Evolutionary structural optimization for dynamic problems. *Comp. & Struct.* **58**, 1067–1073

Xie, Y.M.; Steven, G.P.: 1997 *Evolutionary structural optimization.* Berlin, Heidelberg, New York: Springer

Zhao, C.; Steven, G.P. 1996: Evolutionary natural frequency optimization of thin plate bending vibration problem. *Struct. Optim.* **11**, 244–251

Zhou, M.; Rozvany, G.I.N. 1991: The COC algorithm, Part II: Topological, geometrical and generalized shape optimization. *Comp. Meth. Appl. Mech. Engng.* **89**, 309–336